

Spin dynamics of transitions between muon states

P. F. Meier

Physik-Institut, Universität Zürich, CH-8001 Zürich, Switzerland

(Received 15 October 1981)

The time dependence of the muon spin polarization is calculated for situations where transitions occur between the different (paramagnetic or diamagnetic) muon states which have been observed in semiconductors. It is shown that under suitable experimental conditions the transition rates can be measured with high accuracy.

I. INTRODUCTION

The positive muon is used extensively as a probe in solid-state physics and chemistry. In insulators, semiconductors, and liquids, the muon may bind an electron to form a one-electron atom which can be studied by measuring the time dependence of the muon spin polarization.

Two different paramagnetic muon states have been observed in Si,^{1,2} Ge,³ and diamond.^{4,5} The hyperfine spectrum of the so-called normal muonium state (Mu) is analogous to that of vacuum muonium but with a reduced hyperfine frequency. The observed spectra of the anomalous muonium state (Mu*) are describable by an axially symmetric hyperfine interaction. Besides these two paramagnetic states, the experiments also show that a fraction of the muons are in a diamagnetic state (μ^+) with the muon precessing in the external field with the Larmor frequency.

The amplitudes of the μ SR frequencies for these three states (μ^+ , Mu, Mu*) depend both on temperature and doping concentration.⁶ Recent data on diamond⁵ indicate that at elevated temperatures Mu transforms into Mu*. These experiments initiated the present theoretical investigation of the spin dynamics of transitions among the various muon states.

Analogous transitions are well known in μ SR chemistry. The reaction rates for muonium to form muon-substituted diamagnetic compounds have been determined for a variety of cases.^{7,8} The observation of muonic radicals⁹ has led to extended studies¹⁰ of the reaction mechanisms for muons stopped in liquid unsaturated organic compounds.

If an observed muon state is the reaction product of a transition from an unobserved short-lived precursor state, the amplitudes and phases of precession depend on the reaction rate and the applied field. These dependencies were first calculated by

Ivanter and Smilga¹¹ for transitions $\text{Mu} \rightarrow \mu^+$. Transitions in μ SR chemistry have been studied by Percival and Fischer,¹² and an improved and complete theory of the muon polarization for a general reaction scheme has been developed in Ref. 10.

In the present investigation, the theory is applied to the case of anomalous muonium. New features occur since for Mu* the precession axes of the various frequencies in general do not coincide with the external field. In particular it is shown how the amplitudes and phases depend on the field in the neighborhood of field values for which the frequencies of the precursor and the final state coincide. The occurrence of the predicted phenomena is qualitatively evident; the purpose of the present paper is to provide the quantitative theory of the pertinent spin dynamics and make possible experimental studies of the temperature dependence of reaction rates in detail.

II. EQUATIONS OF MOTION

The spin Hamilton operator for the anomalous muonium state is given by¹³

$$H = \hbar\omega_0 \vec{S}_\mu \cdot \vec{S}_e + \hbar\omega^* (\vec{S}_\mu \cdot \vec{n}) (\vec{S}_e \cdot \vec{n}) - g_\mu \mu_\mu \vec{S}_\mu \cdot \vec{B} - g_e \mu_B \vec{S}_e \cdot \vec{B}, \quad (1)$$

where \vec{n} is a unit vector along the symmetry axis ($a\langle 111 \rangle$ axis in the diamond lattice). It is convenient to introduce the vectors

$$\vec{\omega}_e = -g_e \mu_B \vec{B} / \hbar = 2\pi \cdot 2.802421 \text{ MHz/G} \times \vec{B} \quad (2)$$

and

$$\vec{\omega}_\mu = g_\mu \mu_\mu \vec{B} / \hbar = 2\pi \cdot 0.013553 \text{ MHz/G} \times \vec{B}. \quad (3)$$

The hyperfine parameters ω_0 and ω^* have been determined in Si, Ge, and diamond.⁵ For later

TABLE I. Low-temperature values (Refs. 13 and 15) of hyperfine parameters in units of $2\pi \times 10^6 \text{ s}^{-1}$ for normal muonium (Mu) and anomalous muonium (Mu*) *in vacuo*, Si, Ge, and diamond. The table is from Ref. 5.

	Mu		Mu*		
	ω_0	ω^*	ω_0	ω^*	ω^*
Vacuum	4463	0			
Si	2012	0	92.6		-75.8
Ge	2361	0	130.7		-103.9
Diamond	3711	0	392.5		-560.4

reference their values are summarized in Table I.

The following discussion of the spin dynamics of the system described by Eq. (1) also includes the cases of normal muonium (Mu: $\omega^*=0$) and of the bare muon (μ^+ : $\omega_0=\omega^*=\vec{\omega}_e=0$).

Introducing the Pauli matrices $\vec{\sigma}$ and $\vec{\tau}$ for the muon and electron spin, respectively, the Hamilton operator reads

$$H = \frac{1}{4} \hbar \omega_0 \vec{\sigma} \cdot \vec{\tau} + \frac{1}{4} \hbar \omega^* (\vec{\sigma} \cdot \vec{n}) (\vec{\tau} \cdot \vec{n}) - \frac{1}{2} \hbar \vec{\omega}_\mu \cdot \vec{\sigma} + \frac{1}{2} \hbar \vec{\omega}_e \cdot \vec{\tau}. \quad (4)$$

The density matrix is given by

$$\rho = \frac{1}{4} (1 + \vec{p}_\mu \cdot \vec{\sigma} + \vec{p}_e \cdot \vec{\tau} + p^{jk} \sigma^j \tau^k), \quad (5)$$

where

$$\begin{aligned} \vec{p}_\mu &= \text{Tr}(\rho \vec{\sigma}), \quad \vec{p}_e = \text{Tr}(\rho \vec{\tau}), \\ p^{jk} &= \text{Tr}(\rho \sigma^j \tau^k), \end{aligned} \quad (6)$$

are the muon, electron, and mixed polarizations. The commutation relations

$$[\sigma^j, \sigma^k] = 2i \epsilon_{jkl} \sigma^l \quad (7)$$

and

$$[\sigma^j \tau^m, \sigma^k \tau^n] = 2i (\delta_{j,k} \epsilon_{mnr} \tau^r + \delta_{m,n} \epsilon_{jkl} \sigma^l), \quad (8)$$

and the equation of motion for the density matrix

$$\hbar i \frac{d\rho}{dt} = [H, \rho], \quad (9)$$

lead to the following set of equations for the polarizations:

$$\frac{dp_\mu^j}{dt} = \epsilon_{jkl} \left[\frac{\omega_0}{2} p^{lk} + \frac{\omega^*}{2} p^{lm} n_k n_m - \omega_\mu^k p_\mu^l \right], \quad (10)$$

$$\frac{dp_e^j}{dt} = \epsilon_{jkl} \left[\frac{\omega_0}{2} p^{kl} + \frac{\omega^*}{2} p^{ml} n_k n_m + \omega_e^k p_e^l \right], \quad (11)$$

$$\begin{aligned} \frac{dp^{jk}}{dt} &= \epsilon_{nlm} \left[\delta_{j,m} \delta_{k,n} \frac{\omega_0}{2} (p_\mu^l - p_e^l) \right. \\ &\quad \left. - \delta_{j,n} \left[\frac{\omega^*}{2} n_m n_k p_\mu^l - \omega_\mu^m p^{lk} \right] \right. \\ &\quad \left. + \delta_{k,n} \left[\frac{\omega^*}{2} n_j n_l p_e^m + \omega_e^l p^{jm} \right] \right]. \quad (12) \end{aligned}$$

These 15 equations describe the time evolution in the undisturbed anomalous muonium state. A disturbance due to spin exchange of the bound electron with the surroundings can be accounted for by adding to the right-hand sides of (11) and (12) relaxation terms of the form

$$\begin{aligned} \frac{dp_e^j}{dt} &= \dots - \nu_{\text{ex}} p_e^j, \\ \frac{dp^{jk}}{dt} &= \dots - \nu_{\text{ex}} p^{jk}, \end{aligned}$$

where ν_{ex} is a phenomenologically introduced rate of spin exchange. These kinds of equations have been thoroughly studied by Ivanter and Smilga¹¹ for the case of normal muonium.

The solution of this set of equations may be written as

$$p^\alpha(t) = M^{\alpha\beta}(t) p^\beta(0), \quad (13)$$

with $\alpha, \beta = (1, \dots, 15)$. We are now interested in transformations of a state described by the spin Hamiltonian (1) into a state described by \tilde{H} which has the same structure as (1) but different parameter values (denoted by \sim). This transformation is symbolically denoted by

$$H \xrightarrow{\Lambda} \tilde{H},$$

where Λ is the transformation rate. The time dependence of the polarizations can then be calculated from

$$p_{\text{tot}}^{\alpha}(t) = M^{\alpha\beta}(t)e^{-\Lambda t}p^{\beta}(0) + \tilde{p}^{\alpha}(t), \quad (14)$$

with

$$\tilde{p}^{\alpha}(t) = \Lambda \int_0^t dt' \tilde{M}^{\alpha\beta}(t-t')M^{\beta\gamma}(t')e^{-\Lambda t'}p^{\gamma}(0). \quad (15)$$

This is valid if during the reaction the electron spin polarization is conserved. Conservation of polarization is generally assumed in current theories of radical termination reactions and has been demonstrated in various ESR experiments. The problem of the conservation of electron polarization during reactions of muonium has been discussed extensively by Percival and Fischer.¹²

It is a straightforward numerical task to solve the equations of motion and to evaluate (15) for arbitrary relaxation rates ν_{ex} and directions of \vec{n} and \vec{B} . If U denotes the matrix which diagonalizes M ($U^{-1}MU = D$), the time dependence of the polarizations is given by

$$\tilde{p}^{\alpha}(t) = \tilde{U}_{\alpha\mu} \tilde{U}_{\mu\beta}^{-1} U_{\beta\nu} U_{\nu\gamma}^{-1} p^{\gamma}(0) \Lambda \frac{e^{\tilde{D}_{\mu}t} - e^{D_{\nu}t - \Lambda t}}{\Lambda + \tilde{D}_{\mu} - D_{\nu}}. \quad (16)$$

Expression (16) allows the extension of the work of Ivanter and Smilga¹¹ to include the Mu^* state. This will be discussed elsewhere. In what follows, a simplifying assumption is made that the relaxation effects are negligible ($\nu_{\text{ex}} = 0$). In this case it is unnecessary to work in the Liouville space as has been shown by Fischer *et al.*^{10,12} who developed an elegant and straightforward approach to calculate $\tilde{p}_{\mu}(t)$ for a general reaction scheme. In our notation the muon polarization in the final state is given by

$$\begin{aligned} \tilde{\tilde{p}}_{\mu}(t) &= \Lambda \int_0^t dt' e^{-\Lambda t'} \\ &\quad \times \text{Tr}[e^{-i\tilde{H}(t-t')} \rho(t') e^{i\tilde{H}(t-t')} \vec{\sigma}], \quad (17) \\ \rho(t') &= e^{-iHt'} \rho(0) e^{iHt'}, \end{aligned}$$

where the formal solution of Eq. (9) has been used to describe the time dependence of the density matrix in the precursor and final states. Introducing the eigenvalues and eigenvectors of H ($H|m\rangle = \lambda_m|m\rangle$) and similarly of \tilde{H} , one obtains

$$\begin{aligned} \tilde{\tilde{p}}_{\mu}(t) &= \sum_{\substack{\tilde{m}, \tilde{n} \\ m, n}} \langle \tilde{m} | m \rangle \langle m | \rho(0) | n \rangle \langle n | \tilde{n} \rangle \langle \tilde{n} | \vec{\sigma} | \tilde{m} \rangle \\ &\quad \times \Lambda \int_0^t dt' e^{-\Lambda t'} e^{-i(\tilde{\lambda}_{\tilde{m}} - \tilde{\lambda}_{\tilde{n}})(t-t')} e^{-i(\lambda_m - \lambda_n)t'} \quad (18) \end{aligned}$$

This equation, which has been derived in Ref. 10, has been applied to the determination of the reaction rates of muonic radicals.

In the case of anomalous muonium, the eigenvectors and eigenvalues of H can be evaluated analytically for \vec{n} parallel or perpendicular to \vec{B} . These two cases are discussed in Sec. III along with a few examples of transitions between muon states which are of particular interest for μSR experiments.

III. ANALYTIC SOLUTIONS AND EXAMPLES

A. \vec{n} parallel to \vec{B}

The direction of the field is taken to be the z direction and the equations of motion can be separated. The muon polarization perpendicular to the field oscillates with four transition frequencies:

$$\begin{aligned} \omega_1 &= (\omega_0 + \omega^* + \omega_e - \omega_{\mu} + w)/2, \\ \omega_2 &= (\omega_0 + \omega^* + \omega_e - \omega_{\mu} - w)/2, \\ \omega_3 &= (-\omega_0 - \omega^* + \omega_e - \omega_{\mu} + w)/2, \\ \omega_4 &= (-\omega_0 - \omega^* + \omega_e - \omega_{\mu} - w)/2, \end{aligned} \quad (19)$$

where

$$w = [\omega_0^2 + (\omega_e + \omega_{\mu})^2]^{1/2}. \quad (20)$$

The dependence of these frequencies on B at low fields is shown in Fig. 1 for the hyperfine parameter values appropriate to diamond [$\omega_i(0^\circ)$ refers to anomalous muonium and $\omega_i(\text{Mu})$ to normal muonium]. The eigenvectors associated with the four oscillations are given in the Appendix. Here we just mention the well-known¹⁶ result for the muon polarization

$$\begin{aligned} p_{\mu}^x(t) + ip_{\mu}^y(t) &= \frac{1}{2} \sin^2\chi (e^{i\omega_1 t} + e^{i\omega_3 t}) \\ &\quad + \frac{1}{2} \cos^2\chi (e^{i\omega_2 t} + e^{i\omega_4 t}), \quad (21) \end{aligned}$$

which results if the only nonvanishing¹⁷ initial polarization is $p_{\mu}^x(0) = 1$.

The transition amplitudes depend on the angle χ which is defined by

$$\chi = \frac{1}{2} \arctan \frac{\omega_0}{\omega_e + \omega_{\mu}}. \quad (22)$$

Using the expressions for the time dependence of the polarizations given in Appendix A one can calculate the resulting polarization for a transformation from a precursor state H to a final state \tilde{H}

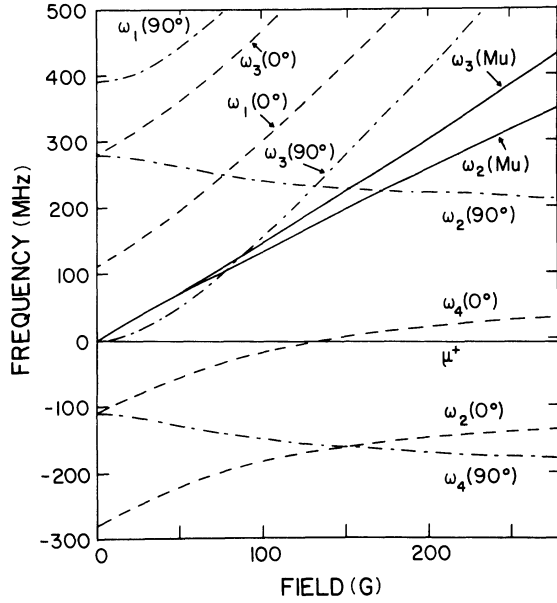


FIG. 1. Frequencies vs transverse field for the hyperfine parameters determined for diamond. Negative values correspond to a negative sense of precession around the field axis. The slope of the Larmor precession frequency ω_μ is -0.01355 MHz/G.

with rate Λ . Neglecting the oscillations of the precursor state at frequencies ω_i , one obtains

$$\tilde{p}_\mu^x(t) = \sum_{i=1}^4 A_i \cos(\tilde{\omega}_i t + \phi_i), \quad (23)$$

where¹⁸

$$A_i \cos \phi_i = \frac{1}{2} \sum_{j=1}^4 W_{ij} \cos^2 \alpha_{ij}, \quad (24)$$

$$A_i \sin \phi_i = -\frac{1}{4} \sum_{j=1}^4 W_{ij} \sin(2\alpha_{ij}).$$

The angles α_{ij} depend on the ratio of the difference of the frequencies and the reaction rate Λ :

$$\tan \alpha_{ij} = \frac{\tilde{\omega}_i - \omega_j}{\Lambda}. \quad (25)$$

The nonvanishing elements of the matrix W are given by

$$\begin{aligned} W_{11} = W_{33} &= \sin \tilde{\chi} \sin \chi \cos(\tilde{\chi} - \chi), \\ W_{22} = W_{44} &= \cos \tilde{\chi} \cos \chi \cos(\tilde{\chi} - \chi), \\ W_{12} = W_{34} &= \sin \tilde{\chi} \cos \chi \sin(\tilde{\chi} - \chi), \\ W_{21} = W_{43} &= -\cos \tilde{\chi} \sin \chi \sin(\tilde{\chi} - \chi). \end{aligned} \quad (26)$$

The frequencies $\tilde{\omega}_i$ and the angle $\tilde{\chi}$ are given by

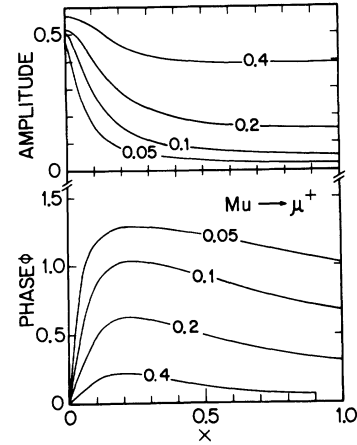


FIG. 2. Amplitude and phase of the muon's Larmor precession with normal muonium as precursor state vs $x = \cot(2\chi)$. The labels on the curves denote the ratio $\Lambda/\omega_0(\text{Mu})$.

the expressions (19)–(22), where according to the Hamiltonian of the final state, ω_0 and ω^* have to be replaced by $\tilde{\omega}_0$ and $\tilde{\omega}^*$. These general formulas allow different transitions to be discussed on the same footing.

As an example we discuss the transitions $\text{Mu} \rightarrow \mu^+$ and $\text{Mu}^*(0^\circ) \rightarrow \mu^+$. For both we have $\tilde{\chi} = 0$ and $\tilde{\omega}_2 = \tilde{\omega}_4 = -\omega_\mu$. The amplitude A and phase ϕ of the final μ^+ frequency are determined from

$$A \cos \phi = \frac{1}{2} \cos^2 \chi (\cos^2 \alpha_2 + \cos^2 \alpha_4) + \frac{1}{2} \sin^2 \chi (\cos^2 \alpha_1 + \cos^2 \alpha_3) \quad (27)$$

and

$$A \sin \phi = \frac{1}{4} \cos^2 \chi [\sin(2\alpha_2) + \sin(2\alpha_4)] + \frac{1}{4} \sin^2 \chi [\sin(2\alpha_1) + \sin(2\alpha_3)], \quad (28)$$

where

$$\tan \alpha_i = \frac{\omega_i + \omega_\mu}{\Lambda}. \quad (29)$$

For the transition $\text{Mu} \rightarrow \mu^+$ the amplitude and phase are plotted in Fig. 2 as a function of $x = \cot 2\chi$ for various values of Λ/ω_0 . These results are already contained in the work of Ivanter and Smilga¹¹ and have been used to interpret measurements in Ge by Kudinov *et al.*¹⁹ In μSR chemistry, this field dependence of the μ^+ amplitude has been used extensively to determine muonium reaction rates.^{20,21} The monotonic decrease of the amplitudes with increasing field is related to the increasing difference of the frequencies of Mu and

μ^+ .

Interesting phenomena are observed by applying the above equations to transitions $\text{Mu}^* \rightarrow \mu^+$. The field dependence of A and ϕ for diamond is plotted in Fig. 3. The strong variation of the phase is due to the change of the differences of frequencies in the precursor and final states. The peak in the amplitude at 120 G corresponds to the crossing of the lines $\omega_4(0^\circ)$ and ω_μ (see Fig. 1).

Equations (23)–(26) can also be used to discuss transitions from μ^+ into Mu or $\text{Mu}^*(0^\circ)$ or from Mu into $\text{Mu}^*(0^\circ)$ or vice versa. Since the frequencies for $\text{Mu}^*(0^\circ)$ and Mu are always different, the latter transitions result in a monotonic dependence of A and ϕ on the field and the transition rate.

B. \vec{n} perpendicular to \vec{B}

If the symmetry axis \vec{n} is perpendicular to the field direction, the spin dynamics are characterized by two angles χ and ψ , which are defined by

$$\tan(2\psi) = \frac{-\omega^*/2}{\omega_e - \omega_\mu} \quad (30)$$

and

$$\tan(2\chi) = \frac{\omega_0 + \omega^*/2}{\omega_e + \omega_\mu} \quad (31)$$

The four transition frequencies observed in a transverse field experiment are then given by

$$\begin{aligned} \omega_1 &= \frac{1}{2} [\omega_0 - \omega^*/2 \csc(2\psi) \\ &\quad + (\omega_0 + \omega^*/2) \csc(2\chi)], \\ \omega_2 &= \frac{1}{2} [\omega_0 - \omega^*/2 \csc(2\psi) \\ &\quad - (\omega_0 + \omega^*/2) \csc(2\chi)], \\ \omega_3 &= \omega_1 - \omega_0, \quad \omega_4 = \omega_2 - \omega_0. \end{aligned} \quad (32)$$

$$p_\mu^y(t) = \frac{1}{2} \sin(\chi + \psi) \sin(\chi - \psi) (\sin\omega_1 t + \sin\omega_3 t) + \frac{1}{2} \cos(\chi + \psi) \cos(\chi - \psi) (\sin\omega_2 t + \sin\omega_4 t). \quad (34)$$

Here and in the following discussion, we have chosen $\vec{n} = (1, 0, 0)$. Other directions are treated in the Appendix.

Since the curves of the frequencies $\omega_2(90^\circ)$ and $\omega_3(90^\circ)$ as a function of B cross those of the triplet muonium (see Fig. 1), it is of interest to investigate the transformation

$$\text{Mu} \rightarrow \text{Mu}^*(90^\circ)$$

in more detail.

The amplitudes and phases of the final-state frequencies [see Eq. (23)] are now given by

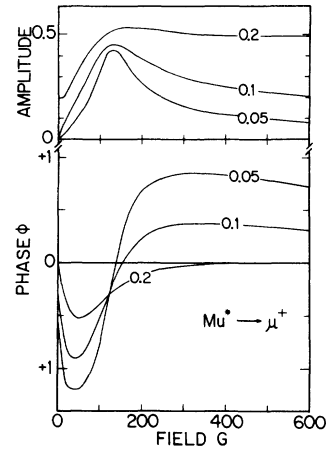


FIG. 3. Amplitude and phase of the muon's Larmor precession with anomalous muonium ($\vec{n} \parallel \vec{B}$) as precursor state vs field. The labels on the curves denote the ratio $\Lambda/\omega_0(\text{Mu}^*)$.

These frequencies are denoted by $\omega_i(90^\circ)$ and are also plotted in Fig. 1 for the case of diamond. The labeling has been chosen such that for $\omega^* = 0$, the ω_i for normal muonium [Eq. (19) with $\omega^* = 0$] are recovered.

The time development of the spin polarization of a muon initially polarized in the x direction and with the field in the z direction is given by

$$\begin{aligned} p_\mu^x(t) &= \frac{1}{2} \sin^2(\chi + \psi) (\cos\omega_1 t + \cos\omega_3 t) \\ &\quad + \frac{1}{2} \cos^2(\chi + \psi) (\cos\omega_2 t + \cos\omega_4 t) \end{aligned} \quad (33)$$

and

$$\begin{aligned} A_i \cos\phi_i &= \frac{1}{2} \sum_{j=1}^4 (W_{ij}^- \cos\tilde{\psi} \cos^2\alpha_{ij}^- \\ &\quad + W_{ij}^+ \sin\tilde{\psi} \cos^2\alpha_{ij}^+) \end{aligned} \quad (35)$$

and

$$\begin{aligned} A_i \sin\phi_i &= -\frac{1}{4} \sum_{j=1}^4 [W_{ij}^- \cos\tilde{\psi} \sin(2\alpha_{ij}^-) \\ &\quad + W_{ij}^+ \sin\tilde{\psi} \sin(2\alpha_{ij}^+)], \end{aligned} \quad (36)$$

with the abbreviations

$$\alpha_{ij}^{\pm} = \arctan \frac{\tilde{\omega}_i \pm \omega_j}{\Lambda} \quad (37)$$

The quantities W_{ij}^{\pm} are given in the Appendix [(A5) and (A6)]. The $\tilde{\omega}_i$ are now to be identified with the frequencies in Eq. (32), whereas the ω_j are the four muonium frequencies [Eq. (19) with $\omega^* \equiv 0$]. In contrast to the case $\vec{n} \parallel \vec{B}$, the precession axes of Mu and $\text{Mu}^*(90^\circ)$ point in different directions. Therefore, the amplitudes and phases of the final state depend on both the differences and sums of $\tilde{\omega}_i$ and ω_j .

In Fig. 4 the amplitudes A_2 , A_3 , and A_4 are plotted versus B for three different values of Λ using the hyperfine parameters of diamond. For small transition rates, A_2 is strongly peaked at 173 G. At this field $\omega_2(\text{Mu}) = \omega_2(\text{Mu}^*)$, and the amplitude is given by $\frac{1}{2} W_{22}^- \cos \psi$. A_3 is maximal at 89 G and A_4 at 117 G. These fields correspond to values where $\omega_3(\text{Mu}) = \omega_3(\text{Mu}^*)$ and $\omega_2(\text{Mu}) = -\omega_4(\text{Mu}^*)$. The amplitudes A_3 and A_4 are weaker than A_2 , which is due to the fact that the electron and mixed polarizations reduce the transition matrix elements W^{\pm} . The phases change sign as the field crosses the values where the amplitudes are maximal.

C. Zero external field

The expressions for the transition $\text{Mu} \rightarrow \text{Mu}^*$ can be considerably simplified in zero external

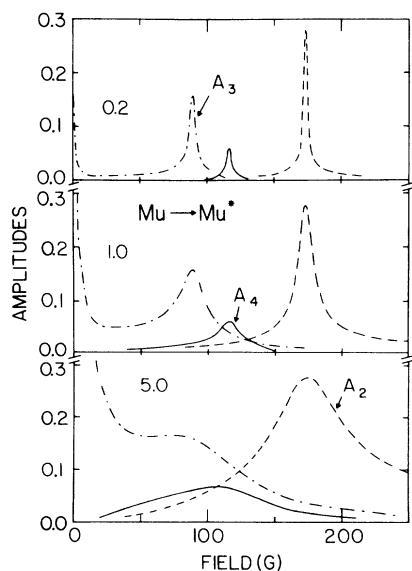


FIG. 4. Amplitudes of $\text{Mu}^*(90^\circ)$ vs field resulting from the transition $\text{Mu} \rightarrow \text{Mu}^*$ for three different values of $\Lambda = 2\pi \times 10^6 \text{ s}^{-1}$ [0.2 (top), 1.0 (middle), 5.0 (bottom)].

field. The \vec{n} pointing in an arbitrary direction, the time dependence of the component of \vec{p}_μ perpendicular to \vec{n} can be obtained from Eqs. (23)–(26):

$$\begin{aligned} \tilde{p}_\mu^\perp(t) = & \frac{1}{2} p_\mu^\perp(0) [A_1^0 \cos(\tilde{\omega}_1^0 t + \phi_1^0) \\ & + A_2^0 \cos(\tilde{\omega}_2^0 t + \phi_2^0)] \quad (38) \end{aligned}$$

For the component parallel to \vec{n} , Eqs. (33)–(36) yield

$$\tilde{p}_\mu^\parallel(t) = \frac{1}{2} p_\mu^\parallel(0) [1 + A_3^0 \cos(\tilde{\omega}_3^0 t + \phi_3^0)] \quad (39)$$

The zero-field frequencies for anomalous muonium are denoted by

$$\begin{aligned} \tilde{\omega}_1^0 &= \omega_0 + \omega^*/2, \\ \tilde{\omega}_2^0 &= \omega^*/2, \\ \tilde{\omega}_3^0 &= \omega_0, \end{aligned} \quad (40)$$

and the amplitudes and phases can be determined from

$$\begin{aligned} A_i^0 \cos \phi_i^0 &= \cos^2 \alpha_{ii}, \\ A_i^0 \sin \phi_i^0 &= -\frac{1}{2} \sin(2\alpha_{ii}), \end{aligned} \quad (41)$$

where the α_{ii} are given by

$$\begin{aligned} \alpha_{11} &= \arctan \frac{\tilde{\omega}_1^0 - \Omega_0}{\Lambda}, \\ \alpha_{22} &= \arctan \frac{\tilde{\omega}_2^0}{\Lambda}, \\ \alpha_{33} &= \arctan \frac{\tilde{\omega}_3^0 - \Omega_0}{\Lambda}. \end{aligned} \quad (42)$$

Here Ω_0 denotes the hyperfine frequency of normal muonium. As a function of the reaction rate Λ , α_{22} behaves drastically different from α_{11} and α_{33} since it is independent of Ω_0 . This is shown in Fig. 5, where the amplitudes and phases are plotted as a function of Λ/Ω_0 for the hyperfine parameter values of diamond. A distinct behavior of the amplitude A_2 of Mu^* as a function of temperature

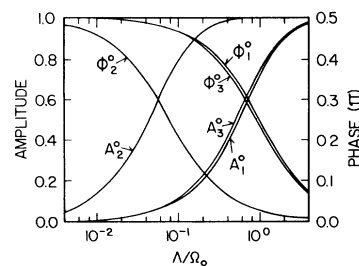


FIG. 5. Amplitudes and phases for the transition $\text{Mu} \rightarrow \text{Mu}^*$ in zero field vs Λ/Ω_0 . The parameter values are those of diamond where $\omega_0(\omega^*)$ is assumed to be positive (negative). For the reversed sign assignment A_3^0 would be below A_1^0 and ϕ_2^0 would be negative.

has recently been observed⁵ in zero-field experiments in diamond. An inspection of Eqs. (41) and (42) shows that the phases ϕ_1^0 and ϕ_3^0 are positive, since Ω_0 is positive and much larger than $|\tilde{\omega}_1^0|$ and $|\tilde{\omega}_3^0|$. The sign of the phase ϕ_2^0 , however, depends on the sign of ω^* , and a measurement of ϕ_2^0 thus determines the signs of ω_0 and ω^* .

IV. CONCLUSIONS

The theory for the spin dynamics of transitions among muon states including anomalous muonium has been discussed. Since the formation of Mu^* in crystals introduces a new axis \vec{n} in addition to the field \vec{B} , a variety of interesting experimental arrangements can be realized. Analytical solutions have been given for special cases which allow a full discussion of all interesting features. In the general case with an arbitrary direction of \vec{n} , no new phenomena occur.

Of particular interest are situations where the frequencies of the precursor and final states are degenerate. Measurements in the neighborhood of these points can yield detailed information about the temperature dependence of the reaction rate. This could also be of interest for investigations of formation rates of muonic radicals in crystals.

Relaxation effects have not been taken into account. They could be included by introducing a phenomenological relaxation frequency ν_{ex} and solving Eq. (16) numerically.

ACKNOWLEDGMENTS

I would like to thank E. Holzschuh, H. Fischer, W. Kündig, B. D. Patterson, and K. Petzinger for

$$p_\mu^x(t) = \frac{1}{2} [\cos^2\gamma \sin^2(\chi + \psi) + \sin^2\gamma \sin^2(\chi - \psi)] (\cos\omega_1 t + \cos\omega_3 t) + \frac{1}{2} [\cos^2\gamma \cos^2(\chi + \psi) + \sin^2\gamma \cos^2(\chi - \psi)] (\cos\omega_2 t + \cos\omega_4 t), \quad (\text{A4})$$

where χ and ψ have been defined in Eqs. (30) and (31). Two angles occur since the precession axes are not along \vec{B} and change their directions with increasing field. The nonzero matrix elements for the transition $\text{Mu} \rightarrow \text{Mu}^*(90^\circ)$ are given by

$$\begin{aligned} W_{13}^+ &= W_{31}^+ = \sin(\chi - \tilde{\chi}) \sin\chi \sin(\tilde{\chi} + \tilde{\psi}), \\ W_{14}^+ &= W_{32}^+ = \cos(\chi - \tilde{\chi}) \cos\chi \sin(\tilde{\chi} + \tilde{\psi}), \\ W_{23}^+ &= W_{41}^+ = -\cos(\chi - \tilde{\chi}) \sin\chi \cos(\tilde{\chi} + \tilde{\psi}), \\ W_{24}^+ &= W_{42}^+ = \sin(\chi - \tilde{\chi}) \cos\chi \cos(\tilde{\chi} + \tilde{\psi}). \end{aligned} \quad (\text{A5})$$

stimulating discussions and critical reading of the manuscript.

APPENDIX

In this appendix the detailed expressions for the eigenvectors and transition matrix elements are collected.

For the case treated in Sec. III A (\vec{n} parallel to \vec{B}) the eigenvectors corresponding to the four frequencies given by Eq. (19) are denoted by F_j :

$$\dot{F}_j = i\omega_j F_j. \quad (\text{A1})$$

They are conveniently expressed as linear combinations of the polarizations:

$$\begin{aligned} F_1 &= -\cos\chi G_1 + \sin\chi G_2, \\ F_2 &= \sin\chi G_1 + \cos\chi G_2, \\ F_3 &= \cos\chi G_3 + \sin\chi G_4, \\ F_4 &= -\sin\chi G_3 + \cos\chi G_4, \end{aligned} \quad (\text{A2})$$

where the mixing angle χ has been defined in Eq. (22) and the G 's are given by

$$\begin{aligned} G_1 &= p_e^x + ip_e^y + p^{zx} + ip^{zy}, \\ G_2 &= p_\mu^x + ip_\mu^y + p^{xz} + ip^{yz}, \\ G_3 &= p_e^x + ip_e^y - p^{zx} - ip^{zy}, \\ G_4 &= p_\mu^x + ip_\mu^y - p^{xz} - ip^{yz}. \end{aligned} \quad (\text{A3})$$

With increasing field the angle χ tends to zero (Paschen-Back region) and the even (odd) eigenvectors and frequencies involve the motion of the muon (electron) spin only.

If \vec{n} is perpendicular to \vec{B} , the amplitudes depend also on the angle between \vec{n} and the initial muon polarization. With $p_\mu^x(0) = 1$ and $\vec{n} = (\cos\gamma, \sin\gamma, 0)$ one gets

and

$$\begin{aligned} W_{11}^- &= W_{33}^- = \cos(\chi - \tilde{\chi}) \sin\chi \sin(\tilde{\chi} + \tilde{\psi}), \\ W_{12}^- &= W_{34}^- = -\sin(\chi - \tilde{\chi}) \cos\chi \sin(\tilde{\chi} + \tilde{\psi}), \\ W_{21}^- &= W_{43}^- = \sin(\chi - \tilde{\chi}) \sin\chi \cos(\tilde{\chi} + \tilde{\psi}), \\ W_{22}^- &= W_{44}^- = \cos(\chi - \tilde{\chi}) \cos\chi \cos(\tilde{\chi} + \tilde{\psi}). \end{aligned} \quad (\text{A6})$$

- ¹J. H. Brewer, K. M. Crowe, F. N. Gygax, R. F. Johnson, B. D. Patterson, D. G. Fleming, and A. Schenck, *Phys. Rev. Lett.* **31**, 143 (1973).
- ²B. D. Patterson, A. Hintermann, W. Kündig, P. F. Meier, F. Waldner, H. Graf, E. Recknagel, A. Weidinger, and T. Wichert, *Phys. Rev. Lett.* **40**, 1347 (1978).
- ³E. Holzschuh, H. Graf, E. Recknagel, A. Weidinger, T. Wichert, and P. F. Meier, *Phys. Rev. B* **20**, 4391 (1979).
- ⁴W. Kündig, *Hyperfine Interactions* **9**, 571 (1981); E. Holzschuh, S. Estreicher, W. Kündig, P. F. Meier, B. D. Patterson, J. P. F. Sellshop, M. C. Stemmet, and H. Appel, *ibid.* **2**, 611 (1981); W. Kündig, E. Holzschuh, P. F. Meier, B. D. Patterson, K. Rüegg, J. P. F. Sellshop, M. C. Stemmet, and H. Appel, *Helv. Phys. Acta* **53**, 611 (1980).
- ⁵E. Holzschuh, W. Kündig, P. F. Meier, B. D. Patterson, J. P. F. Sellshop, M. C. Stemmet, and H. Appel, *Phys. Rev. A* **25**, 1272 (1982).
- ⁶C. Boekema, E. Holzschuh, W. Kündig, P. F. Meier, B. D. Patterson, W. Reichart, and K. Rüegg, *Hyperfine Interactions* **8**, 401 (1981).
- ⁷P. W. Percival, E. Roduner, and H. Fischer, *Adv. Chem Series* **175**, 335 (1979).
- ⁸P. W. Percival and J. Hochmann, *Hyperfine Interactions* **6**, 421 (1979).
- ⁹E. Roduner, P. W. Percival, D. G. Fleming, J. Hochman, and H. Fischer, *Chem. Phys. Lett.* **57**, 37 (1978).
- ¹⁰E. Roduner and H. Fischer, *Chem. Phys.* **54**, 261 (1981).
- ¹¹I. G. Ivanter and V. P. Smilga, *Zh. Eksp. Theor. Fiz.* **54**, 559 (1968) [*Sov. Phys.—JETP* **27**, 301 (1968)].
- ¹²P. W. Percival and H. Fischer, *Chem. Phys.* **16**, 89 (1976).
- ¹³We follow the notation of Ref. 14, which in the present context is more convenient than that of Ref. 5, where the hyperfine parameters $A_{||} = \omega_0 + \omega^*$ and $A_{\perp} = \omega_0$ have been used.
- ¹⁴P. F. Meier, in *Exotic Atoms 79*, edited by K. Crowe *et al.* (Plenum, New York, 1980).
- ¹⁵Experimentally only the relative sign of ω_0 and ω^* is known. For definiteness, ω_0 is assumed to be positive.
- ¹⁶For a tutorial approach see Ref. 14 or A. Hintermann, P. F. Meier, and B. D. Patterson, *Am. J. Phys.* **48**, 956 (1980).
- ¹⁷It is of interest to note that if the electron is initially polarized in direction of \vec{B} , the resulting muon polarization exhibits only two frequencies. This might be of relevance for muonium formation in magnetically ordered materials, where immediately after formation of a paramagnetic state the electron would be coupled to the exchange field.
- ¹⁸It is more meaningful to present the formulas for $A_i \cos \phi_i$ and $A_i \sin \phi_i$ than for A_i and ϕ_i . If the observed frequencies correspond to a muon state which results from several reaction channels n , the total amplitudes and phases can be calculated from
- $$A_i(\text{tot}) \cos \phi_i(\text{tot}) = \sum_{(n)} A_i(n) \cos \phi_i(n).$$
- ¹⁹V. I. Kudinov, E. V. Minaichev, G. G. Myasishcheva, Yu. V. Obukhov, V. S. Roganov, G. I. Savel'ev, and V. G. Firsov, *Zh. Eksp. Teor. Fiz.* **70**, 2041 (1976) [*Sov Phys.—JETP* **43**, 1065 (1976)].
- ²⁰J. H. Brewer, F. N. Gygax, and D. G. Fleming, *Phys. Rev. A* **8**, 77 (1973).
- ²¹P. W. Percival, E. Roduner, and H. Fischer, *Chem. Phys.* **32**, 353 (1978).